TECHNICAL REPORT BRL-TR-3230

BRL

AN INTERMOLECULAR H-O POTENTIAL FOR METHYL ROTATIONS IN SOLID NITROMETHANE

BETSY M. RICE
S. F. TREVINO

APRIL 1991

U.S. ARMY LABORATORY COMMAND

BALLISTIC RESEARCH LABORATORY
ABERDEEN PROVING GROUND, MARYLAND

91 5 06 065

NOTICES

Destroy this report when it is no longer needed. DO NOT return it to the originator.

Additional copies of this report may be obtained from the National Technical Information Service, U.S. Department of Commerce, 5285 Port Royal Road, Springfield, VA 22161.

The findings of this report are not to be construed as an official Department of the Army position, unless so designated by other authorized documents.

The use of trade names or manufacturers' names in this report does not constitute indorsement of any commercial product.

REPORT DOCUMENTATION PAGE			Form Approved OMB No 0704-0188

1. AGENCY USE ONLY (Leave blank)	2. REPORT DATE April 1991	3. REPORT TYPE AND DATES COVERED Final, Jan 90-Dec 90	

4. TITLE AND SUBTITLE	5. FUNDING NUMBERS
An Intermolecular H-O Potential for Methyl Rotations in Solid Nitromethane	1L161102AH43

6. AUTHOR(S)

Betsy M. Rice and S. F. Trevino*

7. PERFORMING ORGANIZATION NAME(S) AND ADDRESS(ES)	8. PERFORMING ORGANIZATION REPORT NUMBER

9. SPONSORING/MONITORING AGENCY NAME(S) AND ADDRESS(ES)	10. SPONSORING/MONITORING AGENCY REPORT NUMBER
U.S. Army Ballistic Research Laboratory ATTN: SLCBR-DD-T Aberdeen Proving Ground, MD 21005-5066	BRL-TR-3230

11. SUPPLEMENTARY NOTES

* S. F. Trevino, AED, ARDEC, Picatinny Arsenal, NJ, and the National Institute of Standards and Technology, Gaithersburg, MD

12a. DISTRIBUTION/AVAILABILITY STATEMENT	12b. DISTRIBUTION CODE
Approved for public release; distribution is unlimited.	

13. ABSTRACT (Maximum 200 words)

A reliable determination of the (H-O) intermolecular potential by which molecules of nitromethane interact with each other is presented. This effort is based upon a very complete body of experimental information which is available on the crystal structure and the rotational properties of the methyl group of the molecule in the solid state. The crystal structure is known in the temperature range of 4 to 233 K. The rotational properties of the methyl group of the molecule have been studied by inelastic neutron scattering with which the energy levels, including the ground state tunnel splitting, have been measured in both the protonated and deuterated samples. These studies provide a most comprehensive characterization of any such similar molecular crystal. The measured properties are directly related to the intermolecular potential, but the inversion of the underlying intermolecular potential from the measured properties has not been straightforward. We describe the application of the principle of maximum entropy in the determination of an intermolecular H-O potential. The resulting potential is of a novel character. At 3.5 GPa, X-ray diffraction studies indicate that the equilibrium orientation of the methyl group in crystalline nitromethane is rotated 45° from the position in the low-temperature ambient pressure form. Calculations of the potential energy as a function of methyl group orientation in crystalline nitromethane at a pressure of 3.5 GPa using the intermolecular potential described herein has reproduced this experimental observation.

14. SUBJECT TERMS			15. NUMBER OF PAGES 31
nitromethane; crystalline nitromethane; solid nitromethane; molecular dynamics; energy surface; intermolecular potential; solid state physics			16. PRICE CODE

17. SECURITY CLASSIFICATION OF REPORT	18. SECURITY CLASSIFICATION OF THIS PAGE	19. SECURITY CLASSIFICATION OF ABSTRACT	20. LIMITATION OF ABSTRACT
UNCLASSIFIED	UNCLASSIFIED	UNCLASSIFIED	SAR

INTENTIONALLY LEFT BLANK.

TABLE OF CONTENTS

INTENTIONALLY LEFT BLANK.

LIST OF FIGURES

INTENTIONALLY LEFT BLANK.

LIST OF TABLES

INTENTIONALLY LEFT BLANK

1. INTRODUCTION

Nitromethane, CH_3-NO_2, has been the subject of several studies which concerned themselves with the rotational properties of the methyl group of this molecule when in the solid-state (Trevino and Rymes 1980; Alefeld et al. 1982; Cavagnat et al. 1985; Cavagnat and Pesquer 1986). The six-fold barrier to rotation of the methyl group about the C-N bond in gas-phase nitromethane has been measured as 0.006 kcal/mol by microwave spectroscopy (Tannenbaum et al. 1954; Tannenbaum, Myers, and Gwinn 1956); the small energy value of this barrier is due to a cancellation of intramolecular interactions which results in a minimal residual intramolecular interaction. In the crystalline phase, however, the activation energy for rotation of the methyl group has been measured as 0.234 kcal/mol (Trevino and Rymes 1980), which suggests that the rotational motion of the methyl group is dominated by intermolecular interactions. Although the molecule is not completely symmetric in the crystal, it is not so distorted as to introduce significant intramolecular interactions into the rotational potential. This study also showed that rotational diffusion of the methyl group occurs by jumps of 120° about the C-N bond axis. X-ray and neutron diffraction determinations of the crystal structure of nitromethane (Trevino, Prince, and Hubbard 1980) show that all methyl groups are equivalent by symmetry and therefore have the same environment. This implies that the internal rotations of all methyl groups are described by a single potential. Therefore, the rotational potential must have three-fold symmetry with respect to a rotation of the methyl group about the C-N bond.

Detailed properties of the rotational potential are reflected in inelastic neutron scattering measurements of many of the torsional energy levels of both the fully protonated and deuterated molecule at 4.2 K and at pressures up to 0.48 GPa (Trevino and Rymes 1980; Alefeld et al. 1982; Cavagnat et al. 1985). Each triply degenerate energy level is split into two tunneling states due to the overlap of the wave functions in the adjacent wells. The amount of splitting is extremely sensitive to the details of the angular dependence of the potential in the region at which the levels exist. The energies at which the levels exist are also dependent on the moment of inertia of the rotating group and can be changed by isotopic substitution of deuterium for hydrogen. The measurements of the tunneling splitting of the ground state and the average position of the first two excited torsional states in each of the two isotopic

samples, as well as the moderate pressure dependence of these levels, have resulted in the formulation of a reliable rotational potential energy function (Cavagnat et al. 1985),

$$V(\theta) = V_3/2[1 - Cos(3\theta)] + V_6/2[1 - Cos(6\theta + \delta)] , \qquad (1)$$

where θ denotes the orientation of the methyl group relative to the heavy atom frame of the nitromethane molecule in the geometry obtained at 4.2 K. We have arbitrarily defined the equilibrium orientation of the methyl group as $\theta = 0°$. Although the form of this potential shows dependence on an intramolecular coordinate, θ, the source of the interactions, which can be described by Equation 1, are predominately intermolecular (Trevino and Rymes 1980; Tannenbaum et al. 1954; Tannenbaum, Myers, and Gwinn 1956). The phenomenological parameters for the potential energy function in Equation 1 which reproduce the spectroscopic measurements are listed in Table 1, and the shape of the potential using these parameters is shown in Figure 1.

The typical form of potential energy functions used in the description of intermolecular interactions are simple functions of interatomic distances. Because it has been determined that the rotational potential in Figure 1 is a result of intermolecular interactions, and assuming that these interactions can be approximated as pairwise additive between atoms of neighboring molecules, it should be possible to describe $V(\theta)$ with simple interatomic functions

$$V(\theta) = \sum_{ij} v[r_{ij}(\theta)] \qquad (2)$$

where $V(\theta)$ is the rotational potential (Figure 1) as a function of the orientation of the methyl group of the molecule about the C-N bond, and $v(r_{ij})$ is the interatomic potential as a function of the separation between the ith hydrogen ($i = 1, 2,$ or 3) of the molecule and the jth atom on a neighboring molecule. We have noted the dependence of r_{ij} on θ in Equation 2 to remind the reader that the interatomic distances between hydrogen atoms and atoms of neighboring molecules are functions of the orientation of the methyl group. There have been previous attempts to formulate pairwise additive interatomic potential energy functions which satisfy Equation 2, with limited success (Cavagnat et al. 1985; Cavagnat and Pesquer 1986). The first attempt (Cavagnat et al. 1985) assumed that the source of the rotational potential was

2

Table 1. Parameters for Potential Energy Functions

Equation 1	
V_3 (eV)	0.0255
V_6 (eV)	-0.0155
δ (degrees)	30.0000
Equation 14	
ϵ (eV)	0.01284000
σ (Å)	2.33722580
a_1 (eV)	-0.07714200
b_1 (Å^{-2})	3.63285690
re_1 (Å)	2.68356980
a_2 (eV)	0.03722530
b_2 (Å^{-2})	2.81809700
re_2 (Å)	3.37513107
r_{cut}(Å)	6.50000000
δr (Å)	0.00100000

due to the interaction between the methyl hydrogens and their neighboring oxygens only. A Lennard-Jones potential

$$v(r) = \epsilon[(\sigma/r)^{12} - (\sigma/r)^6] \tag{3}$$

with $\epsilon = 0.283$ eV and $\sigma = 2.18$ Å was assumed and the calculation of Equation 2 was carried out within the mean field-like approximation; i.e., the calculation of $V(\theta)$ is carried out by rotating the methyl group about the C-N bond without changing the position of the neighbors. This effort produced a $V(\theta)$ which has the qualitative features of the potential in Figure 1. Of equal importance, the pressure dependence of $V(\theta)$ for pressures up to 0.48 GPa and $T = 4.2$ K was well reproduced. Another calculation in which all interatomic interactions were included produce qualitatively similar results (Cavagnat and Pesquer 1986). The latter investigators argue that the $V_3Cos(3\theta)$ term in Equation 1 is due to the H-H interactions and the $V_6Cos(6\theta + \delta)$ term is due to the H-O and H-N interactions. Both studies indicate that the

3

H-O intermolecular interaction is principally responsible for the compound shape of the rotational potential, in particular for the "bump" near the bottom of the well. The shape of $V(\theta)$ is essential for the explanation of the rotational level scheme measured with inelastic neutron scattering and for its pressure dependence up to 0.48 GPa at 4.2 K (Trevino and Rymes 1980; Cavagnat et al. 1985).

Both of the previous calculations of $V(\theta)$ using only intermolecular potential energy functions (Cavagnat et al. 1985; Cavagnat and Pesquer 1986), however, have not been consistent with the crystal structure of nitromethane. Inspection of the rotational potential $V(\theta)$ in Figure 1 reveals that the minimum in energy occurs at $\theta \equiv 20°$. In this figure, as mentioned above, $\theta = 0°$ corresponds to the equilibrium orientation of the methyl group at temperatures from 4.2 K to 150 K as determined by the neutron diffraction study. The pair potentials used in the previous studies give the correct shape for $V(\theta)$, but the minimum is not located at $\theta = 0°$. Therefore, the pair potentials discussed above cannot be said to well represent the interactions in the crystal.

An objection can be raised that the mean field-like approximation is inadequate for the calculation of $V(\theta)$, especially for large values of θ. The calculations of Cavagnat and Pesquer (1986) demonstrate the effect of certain limited reorientations of the neighboring methyl groups on the rotational potential. But certainly near the measured equilibrium orientation (i.e., $\theta = 0°$), the potential must be a minimum.

It is our goal to formulate an intermolecular potential energy function for nitromethane which is consistent with the spectroscopic and structural information available. This paper describes the method and results of this work.

2. POTENTIAL ENERGY SURFACE

All attempts to produce a rotational potential with the shape of that of Figure 1, and with a minimum at $\theta = 0°$ using Lennard-Jones potential energy functions for all atomic species failed. We also used the forms of interatomic potential energy functions based on the work of Caillet and Claverie (1975) and used in the calculations of Cavagnat and Pesquer (1986). We tried to fit Morse functions, as well as other forms of pair potentials in general use, to attain

4

the desired result. Inclusion of electrostatic interactions to these pair potentials made little difference in the results. None of these potential functions were successful in reproducing $V(\theta)$ with a minimum at $0°$; the shape could be reproduced but only with the minimum shifted away from $0°$. Within certain scaling, all of the aforementioned functions generally have the same shape. The failure to obtain the minimum of $V(\theta)$ at $0°$ suggests to us that the shape of the pair potential $v(r)$ as a function of the distance must be changed.

Our task is to rewrite Equation 2 in a form which explicitly exhibits all the experimental information at hand. Reiterating, these include the crystal structure, which defines the distribution of atoms neighboring the methyl group; the spectroscopic measurements of the rotational energy levels, which define the shape of $V(\theta)$; and, again, from the crystal structure, the equilibrium orientation of the methyl group with respect to its heavy atom frame. This can be done in the following manner. From the definition of the Dirac delta function, one can write

$$v(r_{ij}) = \int v(r)\,\delta(r - r_{ij})\,dr \tag{4}$$

so that Equation 2 becomes

$$V(\theta) = \sum_{ij} \int v(r)\,\delta(r - r_{ij})\,dr. \tag{5}$$

The pair distribution function for the neighbors of hydrogen i is defined as

$$\phi_i(r) = \sum_j \delta(r - r_{ij}) \tag{6}$$

from which the desired form of $V(\theta)$ is obtained as

$$V(\theta) = \sum_i \int v(r)\,\phi_i(r[\theta])\,dr. \tag{7}$$

In the preceding equations, we have explicitly assumed one function, $v(r)$, describing a single type of pair interaction which in the present work is the H-O interaction. It is trivial to extend

5

the above arguments to include several different pair potentials, $v(r)$, which would describe interactions of the hydrogens to several atomic species. In Equation 7, the factor $\phi_i(r[\theta])$ expresses the geometric constraints defined by the crystal structure and is, of course, a function of θ.

In practice, Equation 7 is rewritten in an approximate form which allows numerical calculation of the integral. If we define the pair distribution function for the methyl group hydrogens as

$$\Phi(r) = \sum_i \phi_i(r) \tag{8}$$

where the sum is over the three hydrogens of the target molecule, then Equation 7 can be written as:

$$V(\theta_m) = \sum_n v(r_n)\Phi^m(r_n) \tag{9}$$

where

$$r_n = r_{min} + (n - \tfrac{1}{2})\Delta r. \tag{10}$$

The approximation in Equation 9 is that the values of v and Φ at $r = r_n$ are taken as constants over the range of r from $r_{min} + (n-1)\Delta r$ to $r_{min} + (n)\Delta r$. The value of r_{min} (≈ 2.4 Å) corresponds to the minimum value of r_{ij} which occurs in the problem, namely, the minimum H-O distance between a hydrogen of the methyl group and the oxygen of a neighboring molecule. The maximum value of n corresponds to some cutoff in the range of v (≈ 6.5 Å). The value of Δr (0.075 Å) is chosen so as to make the approximation adequate. The superscript m on Φ is included to explicitly indicate that Φ is a function of θ, that is, for each value of θ_m, there corresponds a characteristic distribution function Φ^m. The value of v for each value of n is taken as a free parameter removing the restriction on the form of v as function of r. This problem is not amenable to least squares analyses. Instead, the method of maximum entropy (Gull and Danniel 1979) is used.

6

The method of maximum entropy is a mathematical technique from information theory, often used in image-reconstruction, by which a "best" distribution of a function, for example $v(r_n)$, is obtained subject to constraints which usually reflect limited experimental knowledge. In the present case, this knowledge consists of the shape of $V(\theta_m)$ and the values of $\Phi^m(r_n)$ which are obtained respectively from the spectroscopic and crystallographic studies mentioned above. The reader is referred to Gull and Danniel (1979) for discussions and examples of this powerful method. In the present case, the information theory entropy function (so named because of its functional similarity to the well-known thermodynamic entropy function),

$$ S = -\sum_n v_n \, ln\, (\, v_n/v_n^o\,) \, , \tag{11} $$

is to be maximized subject to the constraint that the parameters v_n be consistent with the set of values of $V(\theta_m)$. This constraint is expressed as the requirement that

$$ \sum_m [\, V(\theta_m) \, - \, V^o(\theta_m)]^2 = 0 \, . \tag{12} $$

We have labelled in short hand v_n as corresponding to $v(r_n)$ in Equation 9 and V^o of Equation 12 are those values of V corresponding to the set of parameters, v_n^o. Satisfaction of these conditions leads to the prescription that a new set of parameters, v_n, is obtained from a previous set, v_n^o, by

$$ v_n = v_n^o \exp\left(\sum_m \left\{ \Phi^m(n) \times \left[\, V(\theta_m) \, - \, V^o(\theta_m)\right]\right\}\right). \tag{13} $$

The meaning of $\Phi^m(n)$ is clear from inspection of Equation 9.

In the initial attempt to obtain a satisfactory set of v_n, a small cluster of nitromethane molecules consisting of the target molecule and its 18 nearest neighbors was used (denoted Model I). The molecule geometry is that given in Table 2 of Trevino, Prince, and Hubbard (1980). The starting set of v_n^o used was obtained from Equation 3 and the parameters ε and σ given there. Details of the procedure require a choice of the number of values of θ_m used to

describe V and the value of Δr used to enumerate the number of v_n. Trial and error resulted in the use of 60 equally spaced values of θ from -60° to 60° and $\Delta r = 0.075$ Å. New sets of v_n were obtained using the procedure of Equation 13 in an iterative manner until a satisfactory convergence of Equation 12 was obtained. The result of this procedure is shown in Figure 2a. The solid line denotes the original $v(r)$ from Equation 3 and the dashed line shows the final set of $v(r)$. The "noise" in the results (the dashed line) is probably due to the approximation to v in Equation 9. The resulting $V(\theta)$ satisfied the requirements that the shape be that of Figure 1 and the minimum of energy be at $\theta = 0°$. A more useful result for analysis than Figure 2a is the difference between the original Lennard-Jones potential and the final $v(r)$ produced by the maximum entropy exercise, shown in Figure 2b (solid line). Although these results are noisy, the curve suggests that the "true" $v(r)$ should be more attractive than the original Lennard-Jones potential from 2.6–3.2 Å, and should have a "bump" at approximately 3.3 Å and perhaps another "bump" at 4.2 Å. A function $v(r)$ was, at this point, constructed which consisted of the original Lennard-Jones potential plus several Gaussian functions, the sum of which was a result of a least-squares fit to the result of the maximum entropy calculation. The $V(\theta)$ obtained from this $v(r)$ using Equation 2 was found to be a rather poor reproduction of the desired result. We are forced to conclude that the maximum entropy technique, as used in the present case, produces only a guide to the desired result. When, however, using the exact expression (Equation 2) and non-linear least-squares fitting to further adjust the parameters of the Gaussian-corrected Lennard-Jones (GCLJ) potential in order to produce the desired $V(\theta)$, we obtained a $v(r)$ shown in Figure 2c (dashed line). The difference between the resulting GCLJ potential and the original Lennard-Jones potential are shown in Figure 2b (dashed line). This potential energy function gives exactly the desired $V(\theta)$ with its minimum at 0°. Note that the GCLJ potential is indeed more attractive than the original Lennard-Jones potential in the range 2.6–3.1 Å, requires a "bump" at approximately 3.5 Å but does not require a "bump" at 4.2 Å. The changes suggested by the maximum entropy procedure were quite accurate.

The nitromethane molecules used in the maximum entropy calculation are not perfectly symmetric as they are in the gas phase. We do not know the deformation of each molecule in the crystal as a function of orientation of the methyl group, except at the equilibrium position. In order to facilitate subsequent Monte Carlo and molecular dynamics simulations, we made the following assumptions about our crystal model in the next stage of the

refinement of the potential energy func n. First, we decided to use a perfectly symmetric molecule to construct the new crystal. Rather than use the raw data from Table 2 of Trevino, Prince, and Hubbard (1980), we used the thermally corrected internal coordinates given in Table 3 of this same reference. In that table, the two O-N bond distances and CNO angles differ slightly. We chose to use the average value of these coordinates in constructing our new model (Model II, Table 2). The potential shown in Figure 2c suggests that interactions beyond 6.5 Å can be neglected. Therefore, we require the potential energy function to have a cutoff at 6.5 Å. We used a crystal model which was large enough to include all H-O pairs within a distance of 6.5 Å to the target molecule. Again, a least-squares fitting procedure is used to obtain the parameters of this potential. The final form of the O-H potential which gave the desired results using this model is

$$
v(r) = \begin{cases}
\varepsilon[(\sigma/r)^{12} - (\sigma/r)^{6}] + \sum_{n=1}^{2} a_n \exp(-b_n[r - re_n]^2), & r < r_{cut} - \delta r \\
\sum_{i=3}^{5} c_i[r - (r_{cut} + \Delta r)]^i, & r_{cut} - \delta r \leq r \leq r_{cut} + \delta r \\
0.0 & r > r_{cut} + \delta r
\end{cases}
\tag{14}
$$

and is shown as a function of H-O distance in Figure 3. The quintic spline function, the second expression in Equation 14, was used to make the potential continuous at its cutoff. The parameters c_3, c_4, and c_5 are determined by requiring that $v(r)$ and its first and second derivatives be continuous at $r = r_{cut} - \delta r$ and $r = r_{cut} + \delta r$. Note that the potential for this crystal model is very similar in shape to that for Model I (Figure 2c); the well and "bump" are located in the same positions, 2.6 and 3.5 Å, respectively. Figure 4 shows the desired $V(\theta)$ with the minimum at 0° (solid line) and the $V(\theta)$ produced using Equation 14 for the large crystal model (dashed line). The resulting fit is almost perfect. It is difficult to imagine any procedure other than the maximum entropy which would have allowed the discovery of the peculiar shape of $v(r)$ arrived at here. The "bump" at 3.5 Å of the H-O potential appears to be absolutely necessary in reproducing $V(\theta)$ with the minimum at 0°. Parameters for the potential function shown in Equation 14 are listed in Table 1.

Table 2. Crystal Models[a]

	Model I[b]	Model II[b]	Model III[c]
R(CH)	1.0739	1.0981	1.000
R(CH)	1.0741	1.0981	1.000
R(CH)	1.0734	1.0981	1.000
R(CN)	1.4805	1.4810	1.470
R(ON)	1.2093	1.2160	1.235
R(ON)	1.2228	1.2160	1.235
θ(HCH)	111.2170	111.6000	109.171
θ(HCH)	111.2061	111.6000	109.171
θHCH)	111.2491	111.6000	109.171
θ(CNO)	118.9326	118.3500	119.150
θ(CNO)	117.7878	118.3500	119.150

[a]Bond distances and angles are given in units of Å and degrees, respectively.
[b]Trevino, Prince, and Hubbard (1980).
[c]Cromer, Ryan, and Schiferl (1985).

3. DISCUSSION

It is difficult to speculate on the origin of the various features (especially that at 3.5 Å) of the final H-O potential except to recognize that many effects may be hidden within the approximation that the H-O interaction is a pairwise additive two-body interaction. Possibly, a quantum mechanical calculation on a large cluster of nitromethane molecules might shed light on the origin of such a potential but it is our understanding that such a calculation is not possible at this time. The only way we can ascertain whether this potential is useful is to determine whether it reproduces experimental measurements.

The energy levels of a one-dimensional methyl rotor can be calculated (Herschbach 1950) for a rotational potential of the form of Equation 1. The measured and calculated energy levels are given in Table 3. The difference between the calculated levels of Cavagnat et al.

Table 3. Torsional Energy Levels of Solid Nitromethane[a]

Isotope	Ground State Tunnel Splitting (μeV)			First Excited State (meV)			Second Excited State (meV)		
	Meas.	Calc.		Meas.	Calc.		Meas.	Calc.	
		Cavagnat[b]	This Work[c]		Cavagnat[b]	This Work[c]		Cavagnat[b]	This Work[c]
CH_3NO_2	35	34	29.5	6.7	6.9	6.7	17.5	16.7	16.4
CD_3NO_2	1.7	1.3	1.	5.3	5.2	5.1	10.6	11.4	11.1

[a] 4.2 K Ambient pressure
[b] Model I, Cavagnat et al. (1985)
[c] Model II

(1985) and the present results are primarily due to the different geometries of the molecules used in these studies. In Cavagnat et al. (1985), the molecular geometry is that revealed in the diffraction measurements where here a symmetric molecule (Model II) is used as discussed above. However, there is still good agreement with the experimental measurements at 4.2 K and low pressure for both the protonated and deuterated species.

The crystal structure of nitromethane at room temperature and pressures up to 6 GPa has been investigated with single crystal X-ray diffraction (Cromer, Ryan, and Schiferl 1985). Several results of that study which are relevant to the present work are: (1) the space group under these conditions is the same as that at 4.2 K and ambient pressure; (2) the hydrogen atom positions were not located at pressures below 3.5 GPa; (3) at 3.5 GPa, the hydrogen positions were attainable from the measurements, and the methyl group is found to be rotated about the C-N bond by an angle of 45° relative to the orientation obtained at 4.2 K. The values of the lattice constants as functions of pressures are given in this work, as well as internal coordinates of the nitromethane molecule at room temperature. The only data which give all internal coordinates at ambient temperatures in this work are at 3.5 GPa, assuming C-H and H-H bond distances of 1.0 and 1.63 Å.

These observations should provide a useful test of the pair potential obtained here. The crystal model used for this purpose (Model III) is constructed from the coordinates in Table 3,

(Cromer, Ryan, and Schiferl 1985) at 3.5 GPa. The values of the internal coordinates used in this model are listed for convenience in Table 2. The effect of pressure was simulated by using the lattice constants specific to the pressures reported in Table 1 of Cromer, Ryan, and Schiferl (1985), shown in Table 4.

The rotational potential, $V(\theta)$, at each pressure was first calculated with all methyl groups in the crystal rotating in phase with the target molecule. This was used to obtain the location of the minimum of $V(\theta)$ at each pressure and therefore the equilibrium orientation of the methyl group predicted by $v(r)$. The location of the minimum at each pressure is given in Table 5. Once this minimum was determined, all surrounding neighbors of the target methyl group were oriented at this rotation angle θ. The mean field-like approximation was then applied and the methyl group of the target molecule was rotated while the neighbors remained fixed. The resulting $V(\theta)$ at each pressure was calculated and the results are shown in Figure 5. Cromer et al. (1985) give two sets of crystallographic data for P = 3.5 GPa, which are labelled as XTL1 and XTL2. Note that the calculated minima of the rotational potentials for XTL1 and XTL2 are 45° and 47° from the orientation of the methyl group at 4.2 K (ambient pressures), in excellent agreement with the reported structures at 3.5 GPa (Cromer, Ryan, and Schiferl 1985).

Cromer et al. (1985) also suggest that at pressures below 0.6 GPa, the methyl groups in the crystal are rotating freely at room temperature. At intermediate pressures, the methyl group is slightly hindered and, at 3.5 GPa, the methyl group is fixed in place. Without dynamics calculations, we cannot conclusively state whether our model O-H potential function will verify these findings. We think it useful, however, to examine the energy difference of the maximum and minimum (the classical barrier height) of the calculated $V(\theta)$ at each pressure. Figure 6 shows the calculated barrier heights from 0.3 to 3.5 GPa (denoted by filled circles). The dashed line corresponds to room temperature. The barrier heights for pressures greater than 3.5 GPa were omitted from this figure because the large magnitudes (4.1, 7.1, and 26.3 eV for 4.0, 5.45, and 6.0 GPa, respectively) obscure the details of the figure in the low pressure region. At pressures up to 2.0 GPa, the classical barrier heights are near room temperature, suggesting that at these pressures the methyl group is indeed a free rotor (or perhaps only slightly hindered). At 3.5 GPa, the classical barrier height is almost 0.45 eV, well above room temperature. Clearly, at this pressure the methyl group is unable to traverse

12

Table 4. Crystallographic Data for Nitromethane at Various Pressures[a]

	0.3	0.33	0.6	1.0	2.0	3.5[b]	3.5[c]	4.0	5.45	6.0
a (Å)	5.182	5.192	5.140	5.090	4.994	4.890	4.884	4.817	4.769	4.730
b (Å)	6.259	6.278	6.191	6.115	5.994	5.885	5.878	5.791	5.777	5.720
c (Å)	8.645	8.675	8.553	8.464	8.272	8.099	8.116	8.039	7.958	7.933

[a] Cromer, Ryan, and Schiferl (1985)
[b] XTL1
[c] XTL2

Table 5. Location of Calculated Minima[a] of $V(\theta)$ at Various Pressures[b]

P(GPa)	θ (Degrees)
0.30	-10.0
0.33	-11.0
0.60	- 7.0
1.00	60.0
2.00	-12.0
3.50 XTL1	-45.0
3.50 XTL2	-47.0
4.00	-55.0
5.45	-52.0
6.00	-54.0

[a] Relative to orientation of methyl group at 4.2 K, 1-bar measurements (Trevino, Prince, and Hubbard 1980)
[b] Model III

the torsional barrier and fully rotate, in agreement with experiment (Cromer, Ryan, and Schiferl 1985).

These calculations of $V(\theta)$ as a function of pressure reveal an additional experimental opportunity. At room temperature, the calculated shape of $V(\theta)$ changes drastically for pressures between 0.3 and 2 GPa (Figure 5). These changes are very sensitive to the form of $v(r)$ as revealed by comparisons between the results presented in Figure 5 and those produced with the Lennard-Jones potential of Equation 6. The mass distribution of deuterium nuclei under these conditions of temperature and pressure should be related to the shape of $V(\theta)$. This mass distribution should be measurable with neutron diffraction and such measurements are planned in the near future.

The success we have had in reproducing several experimental observations using the O-H potential energy function obtained by the maximum entropy exercise has greatly enhanced our confidence in this potential. The intermolecular field which defines the crystal of nitromethane most probably includes at a minimum additional interactions between the hydrogen atoms and atomic species other than the oxygen atoms. An effort is presently underway to determine these with criteria similar to those used in the present work. We also intend to incorporate intramolecular terms in order to carry out fully-dimensional molecular dynamics calculations. In addition, the phase diagram as a function of pressure and temperature will be investigated with Monte Carlo calculations in a search for interesting but as yet unknown phenomena. We proceed with some confidence that a major part of the problem is well in hand.

14
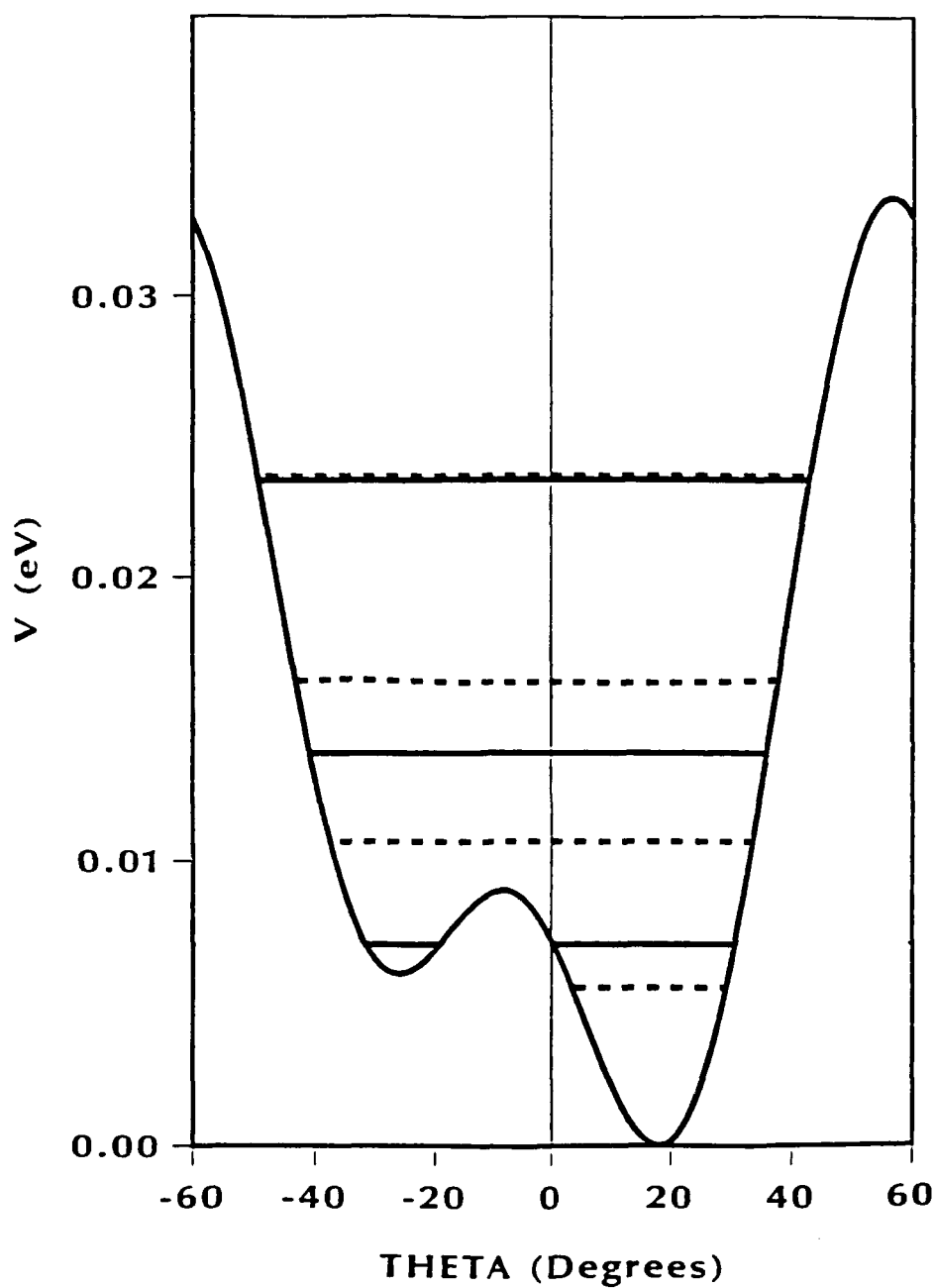
Figure 1. The Rotational Potential as a Function of Methyl Rotation With Parameters Corresponding to 1 Bar (See Equation 1). The Positions of the Average of Each Tunnel Split Energy Level are Shown for CH_3NO_2 (solid lines) and CD_3NO_2 (dashed lines).

15
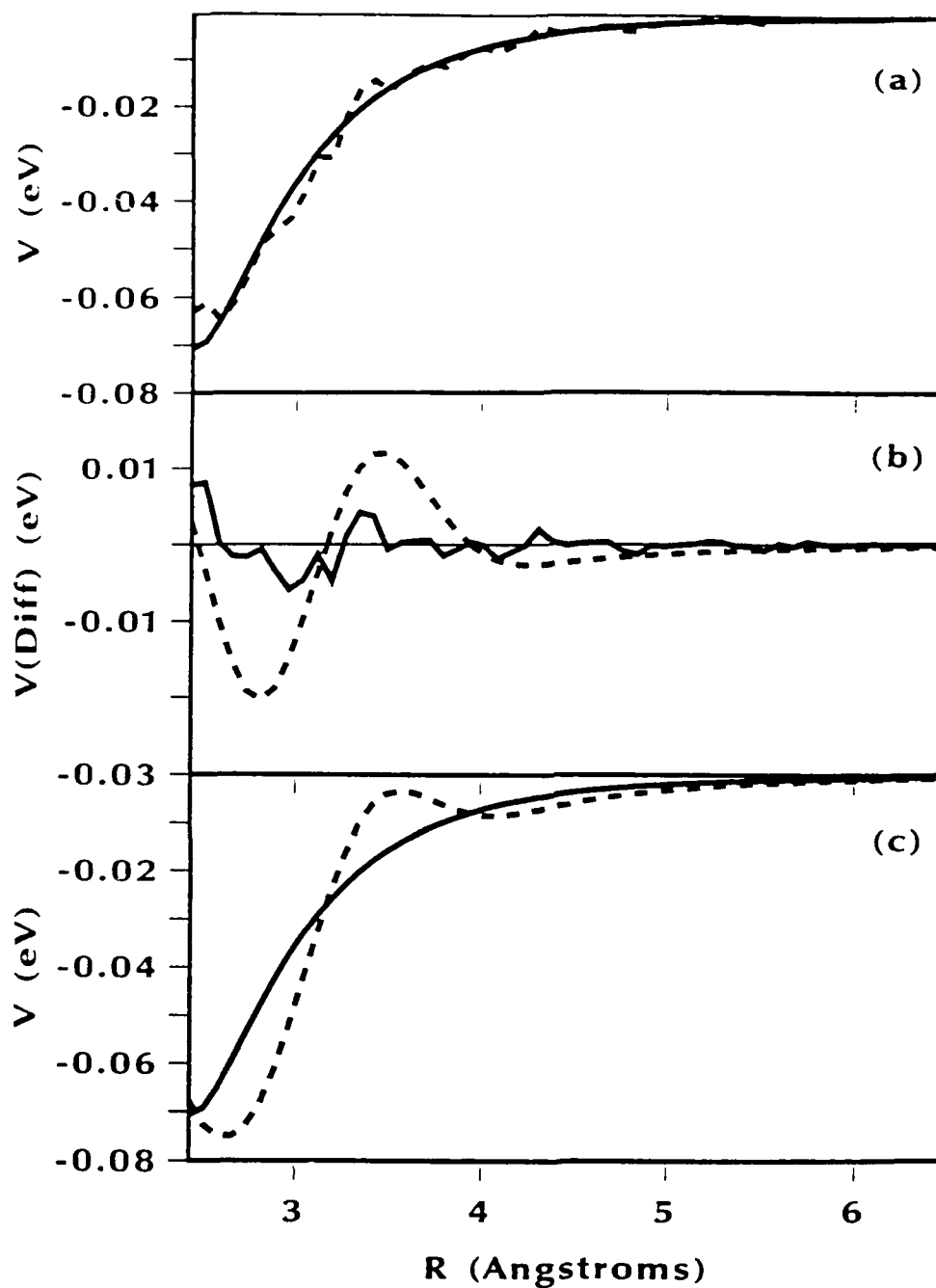
Figure 2. (a) Lennard-Jones H-O Interaction Potential Used in Cavagnat et al. (1985) (Solid Line) and H-O $v(R)$ Predicted From Maximum Entropy Exercise (Dashed Line); (b) Difference Between Lennard-Jones H-O Potential Used in Cavagnat et al. (1985); and H-O $v(r)$ Predicted From Maximum Entropy Exercise (Solid Line) and GCLJ H-O Potential (Dashed Line); (c) Lennard-Jones H-O Interaction Potential Used in Cavagnat et al. (1985) (Solid Line) and GCLJ H-O Potential (Dashed Line).
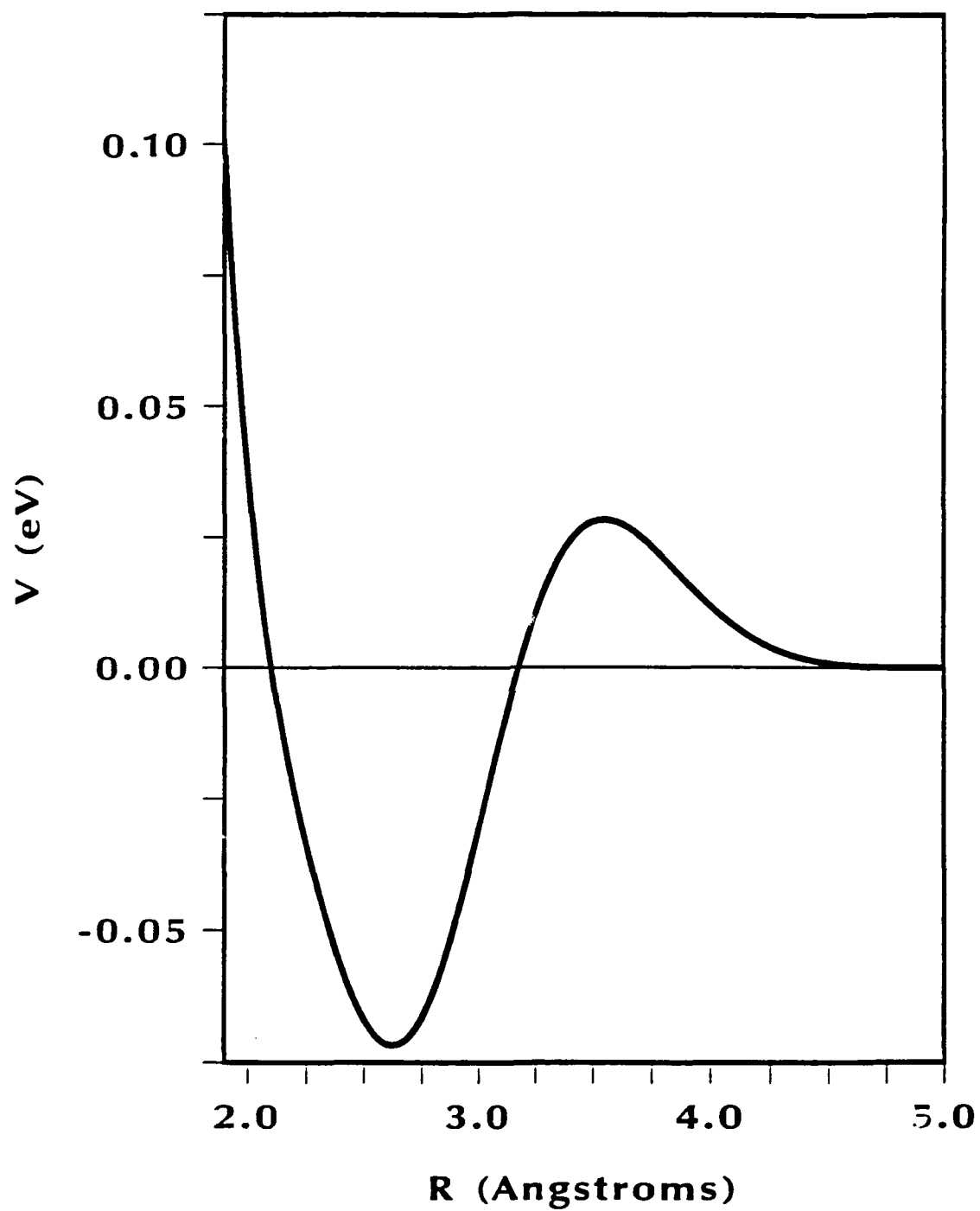
Figure 3. Potential Energy (Equation 14) as a Function of O-H Internuclear Distance.
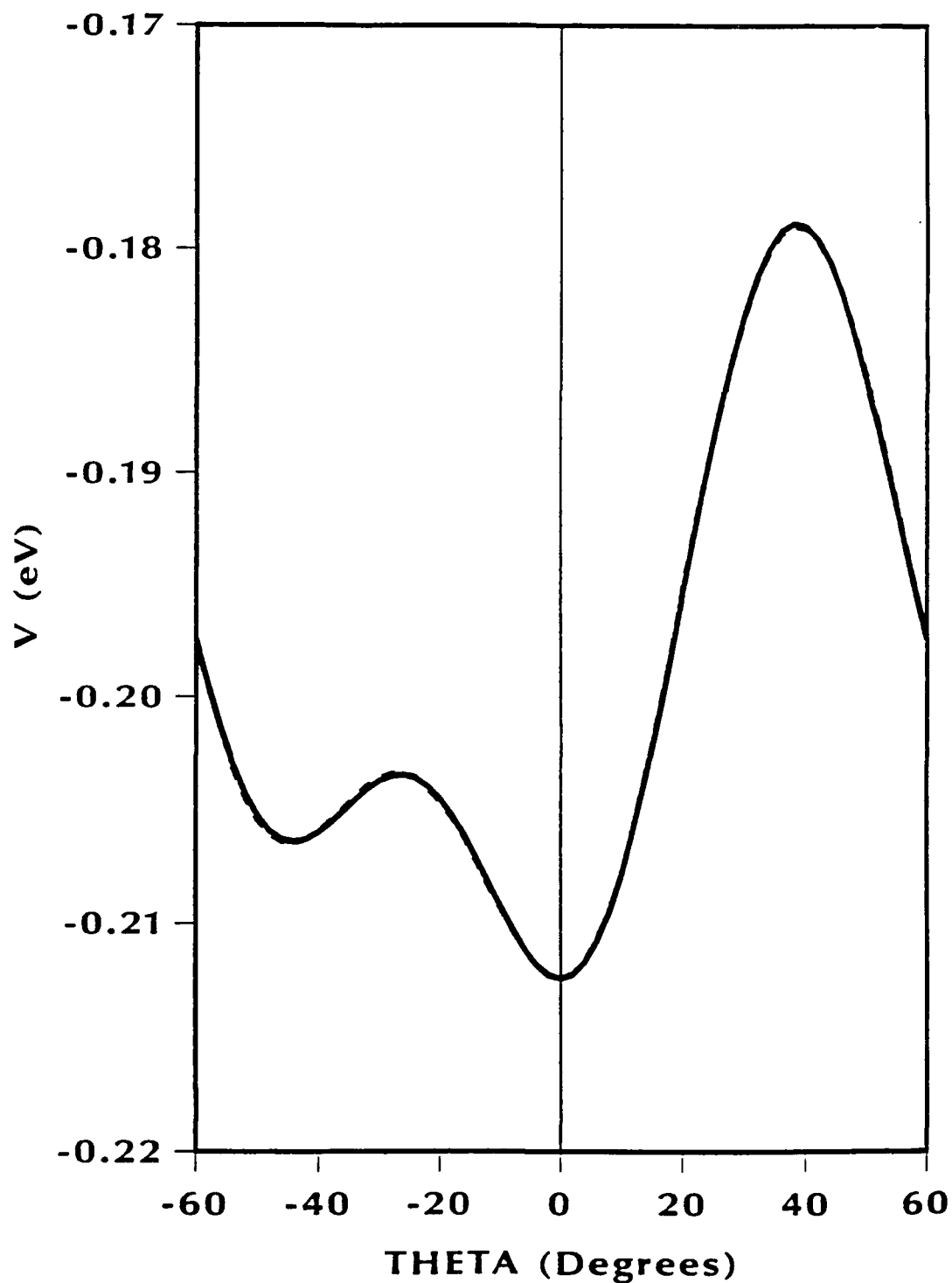
Figure 4. Rotational Potential as a Function of Methyl Rotation. The Solid Curve is Generated by Equation 1 (and Shifted by Approximately 20°) and the Dashed Curve is Generated by All O-H Interactions in Model II Using Internuclear Potential Described in Equation 14.

18
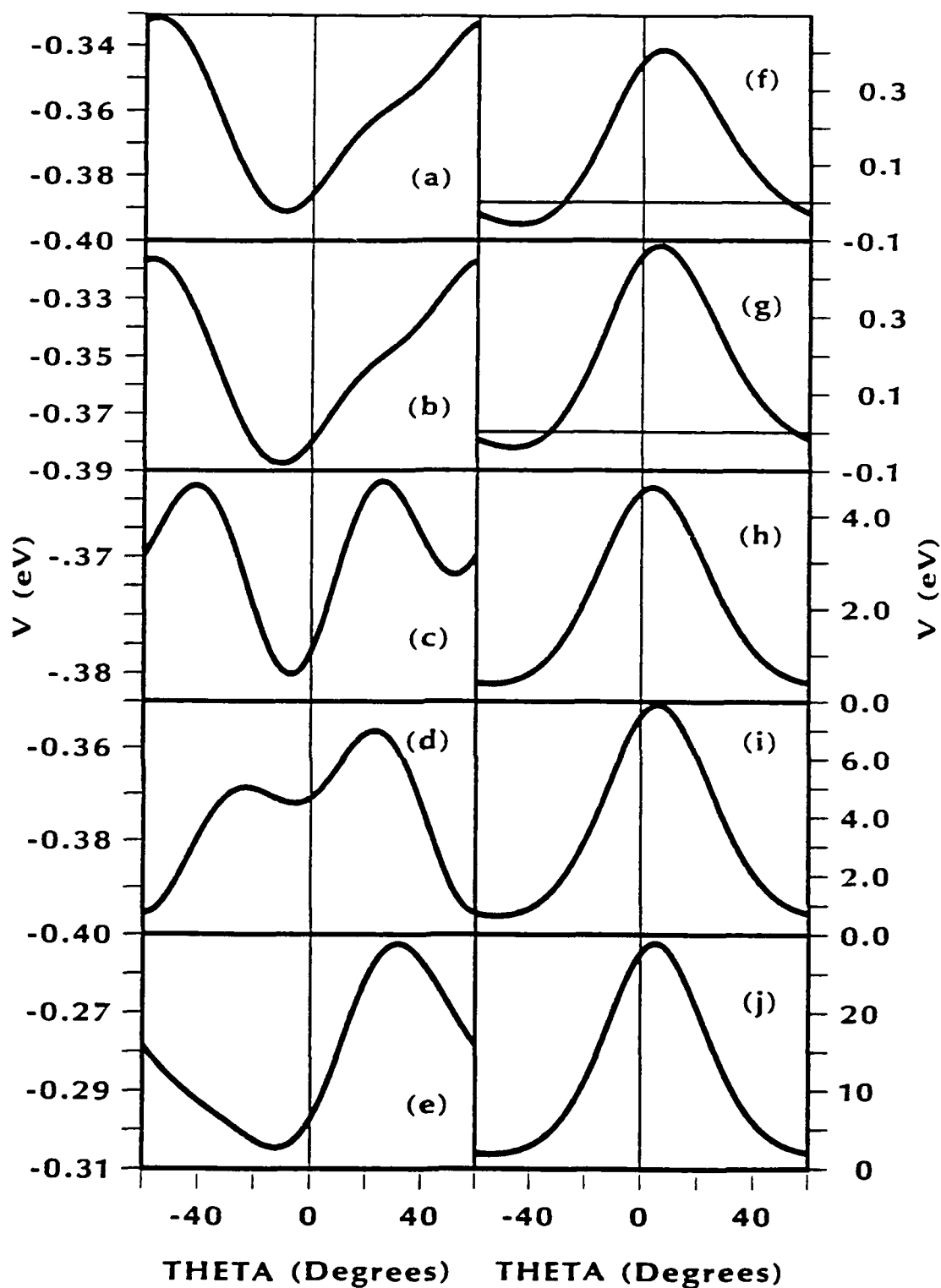
Figure 5. Rotational Potential as a Function of Methyl Rotation at (a) 0.3 GPa, (b) 0.33 GPa, (c) 0.6 GPa, (d) 1.0 GPa, (f) 3.5 GPa (XTL1), (g) 3.5 GPa (XTL2), (h) 4.0 GPa, (i) 5.45 GPa, (j) 6.0 GPa Using Model III.

19
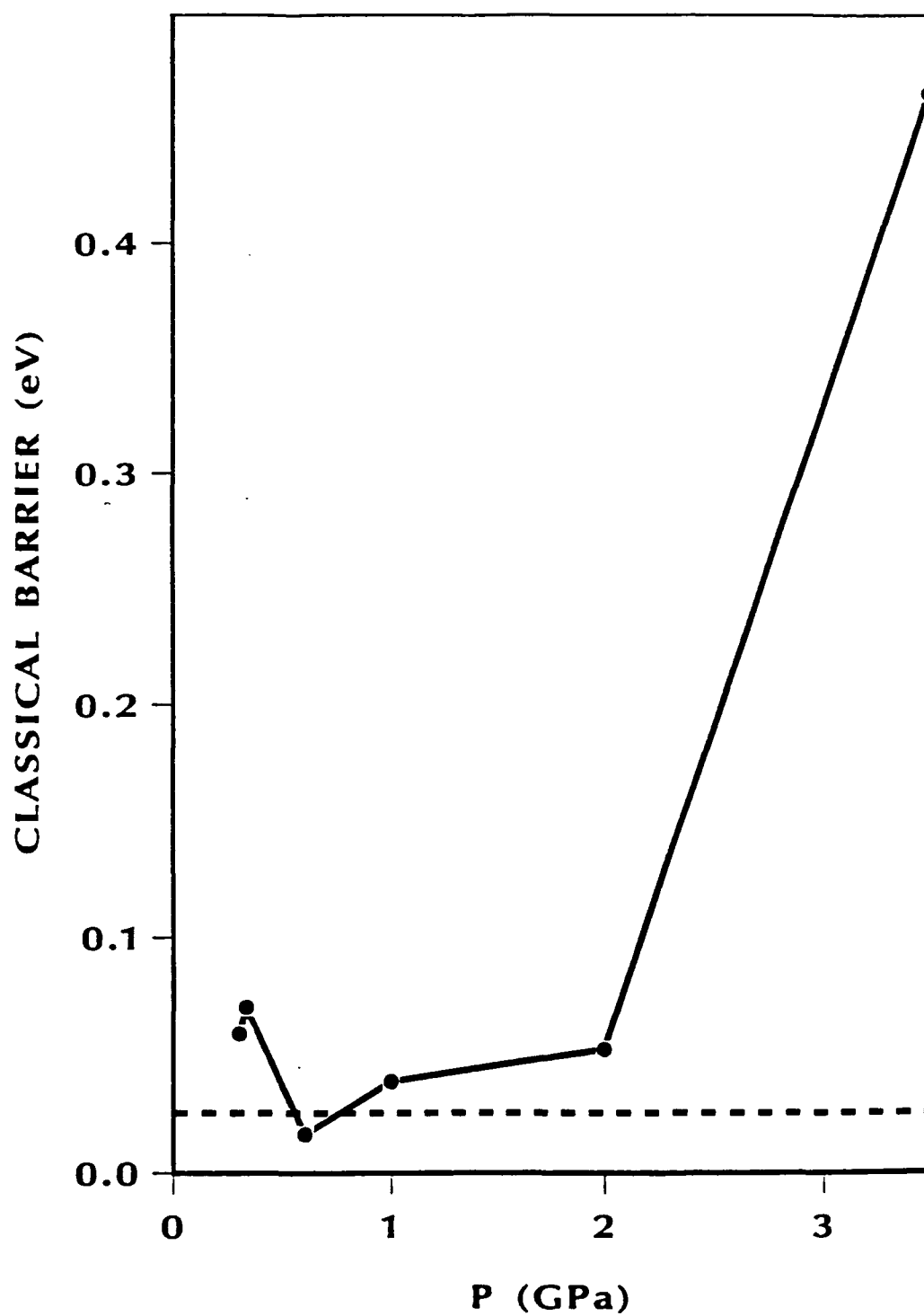
Figure 6. <u>Classical Barrier Height of Rotational Potential as a Function of Pressure.</u>

4. REFERENCES

Alefeld, B., I. S. Anderson, A. Heidemann, A. Magerl, and S. F. Trevino. Journal of Chemical Physics. Vol. 76, p. 2758, 1982.

Caillet, J., and P. Claverie. Acta Crystallographica. Section A: Crystal Physics, Diffraction, Theoretical and General Crystallography. Vol. 31, p. 448, 1975.

Cavagnat, D., A. Magerl, C. Vettier, I. S. Anderson, and S. F. Trevino. Physical Review Letters. Vol. 54, p. 193, 1985.

Cavagnat, D., and M. Pesquer. Journal of Physical Chemistry. Vol. 90, p. 3289, 1986.

Cromer, D. T., R. R. Ryan, and D. Schiferl. Journal of Physical Chemistry. Vol. 89, p. 2315, 1985.

Gull, S. F., and G. J. Danniel. Nature. Vol. 272, p. 686, 1978.

Herschbach, D. R. Journal of Chemical Physics. Vol. 31, p. 91, 1959.

Jaynes, E. T. The Maximum Entropy Formalism. Edited by R. D. Levine and M. Tribus, Cambridge, MA: Massachusetts Institute of Technology, pp. 15–118, 1979.

Tannenbaum, E., R. D. Johnson, R. J. Myers, and W. D. Gwinn. Journal of Chemical Physics. Vol. 22, pp. 949, 1954.

Tannenbaum, E., R. J. Myers, and W. D. Gwinn. Journal of Chemical Physics. Vol. 25, p. 42, 1956.

Trevino, S. F., E. Prince, and C. R. Hubbard. Journal of Chemical Physics. Vol. 73, p. 2996, 1980.

Trevino, S. F., and W. H. Rymes. Journal of Chemical Physics. Vol. 73, p. 3001, 1980.

INTENTIONALLY LEFT BLANK.

23

4   Commander
     US Army Research Office
     ATTN: R. Ghirardelli
              D. Mann
              R. Singleton
              R. Shaw
     P.O. Box 12211
     Research Triangle Park, NC
     27709-2211

2   Commander
     US Army, ARDEC
     ATTN: SMCAR-AEE-B, D.S. Downs
              SMCAR-AEE, J.A. Lannon
     Picatinny Arsenal, NJ   07806-5000

1   Commander
     US Army, ARDEC
     ATTN: SMCAR-AEE-BR, L. Harris
     Picatinny Arsenal, NJ   07806-5000

2   Commander
     US Army Missile Command
     ATTN: AMSMI-RD-PR-E, A.R. Maykut
              AMSMI-RD-PR-P, R. Betts
     Redstone Arsenal, AL   35898-5249

1   Office of Naval Research
     Department of the Navy
     ATTN: R.S. Miller, Code 432
     800 N. Quincy Street
     Arlington, VA   22217

1   Commander
     Naval Air Systems Command
     ATTN: J. Ramnarace, AIR-54111C
     Washington, DC   20360

1   Commander
     Naval Surface Warfare Center
     ATTN: J.L. East, Jr., G-23
     Dahlgren, VA   22448-5000

2   Commander
     Naval Surface Warfare Center
     ATTN: R. Bernecker, R-13
              G.B. Wilmot, R-16
     Silver Spring, MD   20903-5000

5   Commander
     Naval Research Laboratory
     ATTN: M.C. Lin
              J. McDonald
              E. Oran
              J. Shnur
              R.J. Doyle, Code 6110
     Washington, DC   20375

1   Commanding Officer
     Naval Underwater Systems
       Center Weapons Dept.
     ATTN: R.S. Lazar/Code 36301
     Newport, RI   02840

2   Commander
     Naval Weapons Center
     ATTN: T. Boggs, Code 388
              T. Parr, Code 3895
     China Lake, CA   93555-6001

1   Superintendent
     Naval Postgraduate School
     Dept. of Aeronautics
     ATTN: D.W. Netzer
     Monterey, CA   93940

3   AL/LSCF
     ATTN: R. Corley
              R. Geisler
              J. Levine
     Edwards AFB, CA   93523-5000

1   AL/MKPB
     ATTN: B. Goshgarian
     Edwards AFB, CA   93523-5000

1   AFOSR
     ATTN: J.M. Tishkoff
     Bolling Air Force Base
     Washington, DC   20332

1   OSD/SDIO/IST
     ATTN: L. Caveny
     Pentagon
     Washington, DC   20301-7100

1   Commandant
     USAFAS
     ATTN: ATSF-TSM-CN
     Fort Sill, OK   73503-5600

1   F.J. Seiler
     ATTN: S.A. Shackleford
     USAF Academy, CO   80840-6528

No. of
Copies   Organization

1   IBM Corporation
     ATTN: A.C. Tam
     Research Division
     5600 Cottle Road
     San Jose, CA   95193

1   IIT Research Institute
     ATTN: R.F. Remaly
     10 West 35th Street
     Chicago, IL   60616

2   Director
     Lawrence Livermore
       National Laboratory
     ATTN: C. Westbrook
              M. Costantino
     P.O. Box 808
     Livermore, CA   94550

1   Lockheed Missiles & Space Co.
     ATTN: George Lo
     3251 Hanover Street
     Dept. 52-35/B204/2
     Palo Alto, CA   94304

1   Los Alamos National Lab
     ATTN: B. Nichols
              T7, MS-B284
     P.O. Box 1663
     Los Alamos, NM   87545

1   National Science Foundation
     ATTN: A.B. Harvey
     Washington, DC   20550

1   Olin Ordnance
     ATTN: V. McDonald, Library
     P.O. Box 222
     St. Marks, FL   32355-0222

1   Paul Gough Associates, Inc.
     ATTN: P.S. Gough
     1048 South Street
     Portsmouth, NH   03801-5423

2   Princeton Combustion
       Research Laboratories, Inc.
     ATTN: M. Summerfield
              N.A. Messina
     475 US Highway One
     Monmouth Junction, NJ   08852

1   Hughes Aircraft Company
     ATTN: T.E. Ward
     8433 Fallbrook Avenue
     Canoga Park, CA   91303

1   Rockwell International Corp.
     Rocketdyne Division
     ATTN: J.E. Flanagan/HB02
     6633 Canoga Avenue
     Canoga Park, CA   91304

4   Sandia National Laboratories
     Division 8354
     ATTN: R. Cattolica
              S. Johnston
              P. Mattern
              D. Stephenson
     Livermore, CA   94550

1   Science Applications, Inc.
     ATTN: R.B. Edelman
     23146 Cumorah Crest
     Woodland Hills, CA   91364

3   SRI International
     ATTN: G. Smith
              D. Crosley
              D. Golden
     333 Ravenswood Avenue
     Menlo Park, CA   94025

1   Stevens Institute of Tech.
     Davidson Laboratory
     ATTN: R. McAlevy, III
     Hoboken, NJ   07030

1   Sverdrup Technology, Inc.
     LERC Group
     ATTN: R.J. Locke, MS SVR-2
     2001 Aerospace Parkway
     Brook Park, OH   44142

1   Thiokol Corporation
     Elkton Division
     ATTN: S.F. Palopoli
     P.O. Box 241
     Elkton, MD   21921

1   Morton Thiokol, Inc.
     Huntsville Division
     ATTN: J. Deur
     Huntsville, AL   35807-7501

3   Thiokol Corporation
     Wasatch Division
     ATTN: ·S.J. Bennett
     P.O. Box 524
     Brigham City, UT   84302

1   United Technologies Research Center
     ATTN: A.C. Eckbreth
     East Hartford, CT   06108

26

3   United Technologies Corp.
     Chemical Systems Division
     ATTN: R.S. Brown
              T.D. Myers (2 copies)
     P.O. Box 49028
     San Jose, CA   95161-9028

1   Universal Propulsion Company
     ATTN: H.J. McSpadden
     Black Canyon Stage 1
     Box 1140
     Phoenix, AZ   85029

1   Veritay Technology, Inc.
     ATTN: E.B. Fisher
     4845 Millersport Highway
     P.O. Box 305
     East Amherst, NY   14051-0305

1   Brigham Young University
     Dept. of Chemical Engineering
     ATTN: M.W. Beckstead
     Provo, UT   84058

1   California Institute of Tech.
     Jet Propulsion Laboratory
     ATTN: L. Strand/MS 512/102
     4800 Oak Grove Drive
     Pasadena, CA   91009

1   California Institute of
        Technology
     ATTN: F.E.C. Culick/
              MC 301-46
     204 Karman Lab.
     Pasadena, CA   91125

1   University of California
     Los Alamos Scientific Lab.
     P.O. Box 1663, Mail Stop B216
     Los Alamos, NM   87545

1   University of California,
        Berkeley
     Chemistry Deparment
     ATTN: C. Bradley Moore
     211 Lewis Hall
     Berkeley, CA   94720

1   University of California,
        San Diego
     ATTN: F.A. Williams
     AMES, B010
     La Jolla, CA   92093

2   University of California,
        Santa Barbara
     Quantum Institute
     ATTN: K. Schofield
              M. Steinberg
     Santa Barbara, CA   93106

1   University of Colorado at
        Boulder
     Engineering Center
     ATTN: J. Daily
     Campus Box 427
     Boulder, CO   80309-0427

2   University of Southern
        California
     Dept. of Chemistry
     ATTN: S. Benson
              C. Wittig
     Los Angeles, CA   90007

1   Cornell University
     Department of Chemistry
     ATTN: T.A. Cool
     Baker Laboratory
     Ithaca, NY   14853

1   University of Delaware
     ATTN: T. Brill
     Chemistry Department
     Newark, DE   19711

1   University of Florida
     Dept. of Chemistry
     ATTN: J. Winefordner
     Gainesville, FL   32611

3   Georgia Institute of Technology
     School of Aerospace Engineering
     ATTN: E. Price
              W.C. Strahle
              B.T. Zinn
     Atlanta, GA   30332

1   University of Illinois
     Dept. of Mech. Eng.
     ATTN: H. Krier
     144MEB, 1206 W. Green St.
     Urbana, IL   61801

1   Johns Hopkins University/APL
     Chemical Propulsion
        Information Agency
     ATTN: T.W. Christian
     Johns Hopkins Road
     Laurel, MD   20707

27

28

USER EVALUATION SHEET/CHANGE OF ADDRESS

This laboratory undertakes a continuing effort to improve the quality of the reports it publishes. Your comments/answers below will aid us in our efforts.

1. Does this report satisfy a need? (Comment on purpose, related project, or other area of interest for which the report will be used.) _____

_____

_____

2. How, specifically, is the report being used? (Information source, design data, procedure, source of ideas, etc.) _____

_____

_____

3. Has the information in this report led to any quantitative savings as far as man-hours or dollars saved, operating costs avoided, or efficiencies achieved, etc? If so, please elaborate. _____

_____

_____

4. General Comments. What do you think should be changed to improve future reports? (Indicate changes to organization, technical content, format, etc.) _____

_____

_____

BRL Report Number _____BRL-TR-3230_____ Division Symbol _____

Check here if desire to be removed from distribution list. ____

Check here for address change. ____

Current address: Organization _____

Address _____

_____

DEPARTMENT OF THE ARMY

Director
U.S. Army Ballistic Research Laboratory
ATTN: SLCBR-DD-T
Aberdeen Proving Ground, MD 21005-5066

OFFICIAL BUSINESS

BUSINESS REPLY MAIL	**NO POSTAGE**
FIRST CLASS PERMIT No 0001, APG, MD	**NECESSARY**
	IF MAILED
Postage will be paid by addressee	**IN THE**
	UNITED STATES

Director
U.S. Army Ballistic Research Laboratory
ATTN: SLCBR-DD-T
Aberdeen Proving Ground, MD 21005-5066